RSC Advances

PAPER

View Article Online
View Journal | View Issue

Cite this: *RSC Adv.*, 2020, **10**, 14944

A strategy for preparing non-fluorescent graphene oxide quantum dots as fluorescence quenchers in quantitative real-time PCR

Chenyan Hu,†[a] Zhongzhu Yang,†[a] Zhen Song,[a] Linghui Xiao*[b] and Yang He *[a]

In recent years, graphene oxide quantum dots (GOQDs) have emerged as novel nanomaterials for optical sensing, bioimaging, clinical testing, and environmental testing. However, GOQDs demonstrate unique photoluminescence properties, with GOQDs having quantum limitations and edge effects that often affect the accuracy of the test results in the sensory field. Herein, GOQDs with a large content of hydroxyl groups and low fluorescence intensity were first prepared *via* an improved Fenton reaction in this study, which introduces a large amount of epoxy groups to break the C–C bonds. The synthesized GOQDs show no significant variation in the fluorescence intensity upon ultraviolet and visible light excitations. We further utilized the GOQDs as fluorescence quenchers for different fluorescent dyes in real-time fluorescence quantitative polymerase chain reaction (qRT-PCR), and verified that the addition of GOQDs (5.3 μg ml^{-1}) into a qRT-PCR system could reduce the background fluorescence intensity of the reaction by fluorescence resonance energy transfer (FRET) during its initial stage and its non-specific amplification, and improve its specificity. In addition, the qRT-PCR method could detect two different lengths of DNA sequences with a high specificity in the 10^4 to 10^{10} copies per μl range. It is of paramount importance to carry out further investigations to establish an efficient, sensitive, and specific RT-PCR method based on the use of GOQD nanomaterials as fluorescence quenchers.

Received 6th January 2020
Accepted 6th April 2020

DOI: 10.1039/d0ra00142b

rsc.li/rsc-advances

Introduction

Recently, biosensors have been widely studied to be employed in rapid detection methods for pathogens or pathogenic genes in the sensory field.[1,2] In particular, fluorescence sensors with modified fluorophores, which are based on deoxyribonucleic acid (DNA), appear to be promising for application due to their stability, high specificity, and sensitivity.[3,4] Fluorescence sensors to detect the presence of a target molecule are typically based on the fluorescence resonance energy transfer (FRET) process,[5] thus the choice of the receptor pair usually determines the analytical performance of the fluorescence sensor.[6] To reduce the limitations that characterize the receptor pairs, studies have shown that novel nanomaterials, which exhibit an effective quenching ability in a broad range of emission wavelengths, can be used as broad-spectrum quenching molecules.[7–9] For instance, fluorescence sensors based on graphene oxide quantum dots (GOQDs) have been applied in a wide range of fields for cancer research, clinical trials, and medical practice.[10–12]

GOQDs are zero-dimensional materials, which are nanoscale fragments of graphene oxide (GO).[13,14] Due to the quantum confinement and the edge effect, GOQDs have ignited tremendous research interest for their outstanding properties in terms of physical and chemical properties when compared to layered GO. For instance, the quantum limitations and the edge effects of GOQDs can be greatly enhanced to achieve distinctive photoluminescence properties by adjusting the size of the GOQDs and the number of oxygen-containing functional groups.[15] In addition, due to their good biocompatibility, fluorescence stability, and low toxicity, GOQDs are suitable for optical sensing, bioimaging, clinical testing, and environmental testing.[16,17] Nevertheless, the high background fluorescence intensity, which characterizes GOQDs, often affects the accuracy of the test results. Fluorescence sensors usually present a low concentration of GOQDs to improve the accuracy of the detection results.[18] Therefore, it is of pivotal importance to reduce the influence of the background fluorescence of the GOQDs to enable their use in a broader variety of sensing and detection techniques.

Polymerase chain reaction (PCR) is a process that the mimics DNA replication *in vitro* and that can detect a target DNA sequence from the final reaction product.[19] In recent years, a real-time fluorescent quantitative PCR technology (qRT-PCR)

[a]*College of Medical Technology, State Key Laboratory of Characteristic Chinese Medicine Resources in Southwest China, Chengdu University of Traditional Chinese Medicine, Chengdu, 611137, China. E-mail: heyang@cdutcm.edu.cn*

[b]*Hospital of Chengdu University of Traditional Chinese Medicine, Chengdu, 610075, China. E-mail: xiaolh2010@hotmail.com*

† These authors contributed equally to this work.

has been developed based on the traditional PCR. This technique monitors the PCR amplification *via* the variations in the fluorescence intensity.[20] Compared to the traditional PCR, qRT-PCR exhibits a significant advantage to detect the evolution of the amplification reaction by detecting the fluorescence signal in real-time. However, regardless of the dye method or the probe method used, a high background fluorescence intensity is present in qRT-PCR. Moreover, the detection accuracy is lower in the dye method when the primers with poor specificity to the templates.[21,22] Therefore, it is necessary to solve the issue generated by the presence of such high original background fluorescence intensity to improve the specificity of the qRT-PCR method.

Based on the improved Fenton reaction, a graphite layer was initially separated by using MnO_3^+ as the intercalating agent. Successively, the graphene was oxidized into GO by H_2O_2, which contains a large quantity of epoxy functional groups. At this point, the Fenton reaction occurs between the zero-valent iron and H_2O_2. In this fashion, non-fluorescent GOQDs with a large number of hydroxyl groups were obtained. So far, there are no studies about non-fluorescent GOQDs. In this work, we report a new qRT-PCR method that employs easily prepared and non-fluorescent GOQDs to efficaciously enhance the specificity of qRT-PCR reactions. At first, the fluorescence quenching ability of non-fluorescent GOQDs was investigated by combining together various fluorescent dyes. Furthermore, the non-fluorescent GOQDs were applied to qRT-PCR *via* the formation of a π–π stacking and hydrogen bonds between the TaqMan probe and the GOQDs to reduce the original background fluorescence intensity. The π–π stacking and the hydrogen bond between the primers and the GOQDs significantly improved the specificity of qRT-PCR. Moreover, two different lengths DNA fragments (106 bp and 65 bp) were detected *via* qRT-PCR based on the GOQDs. The superior performance of the GOQDs in qRT-PCR indicates that this enables new applications in the biological and medical fields.

Experimental

Reagents and materials

Graphite (crystalline powder, 100 mesh) was purchased from Qingdao Laixi Colloidal Graphite Factory (Qingdao, China). Potassium nitrate (KNO_3), potassium permanganate ($KMnO_4$), sulphuric acid (H_2SO_4), and 30% hydrogen peroxide (H_2O_2) were supplied by Chengdu Kelong Chemical Reagent Factory (Chengdu, China). The 1000 Da dialysis bag was provided by Shanghai Yuanye Biological Science & Technology Company (Shanghai, China). The solutions were prepared by using ultrapure water (>18 MΩ) from the ELGA water purification system (ELGA, London, UK). All the reagents used in this study were of analytical reagent grade.

Improved Fenton reaction

Graphite (0.5 g) was mixed with sulphuric acid (95–98%) and the solution was stirred at room temperature prior to the addition of $NaNO_3$ (0.5 g). Meanwhile, $KMnO_4$ (3 g) was added to the sulphuric acid (95–98%) before adding $NaNO_3$ (0.5 g) to form MnO_3^+. The manganese-embedded graphite was formed by the slow addition of MnO_3^+ into graphite. Successively, H_2O_2 (30%) and zero-valent iron were added into 10 ml of manganese-embedded graphite. The zero-valent iron in the liquid was removed by boiling the solution. The liquid required a continuous addition of H_2O_2 (30%) and was left boiling for 6 min to obtain the GOQDs solution. The experiment was carried out by using a magnetic stirrer. The GOQDs solution was dialyzed (pH 2.0, 1000 Da) for 7 days to remove the excess of Fe^{2+}, Fe^{3+}, the traces of H_2O_2, and of other low-molecular mass reaction products. Finally, a pale yellow transparent GOQDs solution was obtained.

Characterization

Atomic force microscopy (AFM) of the GOQDs was conducted on a Multimode Nanoscope V scanning probe microscopy system (Bruker, USA). In the test, a commercial AFM cantilever tip (Bruker, USA) with a force constant of ~50 N m^{-1} and a resonance vibration frequency of ~350 kHz was used. The X-ray photoelectron spectroscopy (XPS) pattern of the samples was measured by using a Thermo ESCALAB 250XI scanning XPS microscope (a monochromated Al Kα radiant energy of 1486.6 eV). Fourier transform infrared spectroscopy (FT-IR) spectra were obtained on a NICOLET 5700 FT-IR spectrometer (Waltham, USA). The samples to perform the FT-IR measurements were prepared by grinding a dry powder of GOQDs with KBr, which was then compressed into a thin slice. UV-visible absorption spectra were obtained by using a MAPADA UV-6300 ultraviolet-visible spectrophotometer (Shanghai, China). The photoluminescence spectrum (PL) of GO, 6-FAM, JOE, and Cy3 was recorded on a Lengguang F97PRO Fluorescence Spectrophotometer (Shanghai, China). The emission spectrum of GOQDs was obtained by using a detection wavelength of 440 nm and an excitation wavelength of 380 nm. The emitted fluorescence intensity of 6-FAM, JOE and Cy3 were detected by applying excitation wavelengths of 485 nm, 520 nm and 535 nm and emission wavelengths of 525 nm, 548 nm and 556 nm, respectively.

Single-stranded DNA templates and primers

The primers and the probes were designed by employing the Primer Express 3.0.1 software, which was developed based on the related works. All the single-stranded DNA templates and primers were synthesized by Shanghai Sangon Biological Science & Technology Company (Shanghai, China). The specific sequences are listed in Table 1. The single-stranded DNA, primers, probes, and templates were dissolved in a solution of ultrapure water and stored at −20 °C.

Construction of 106 bp plasmid DNA

MicroRNA was extracted from human breast epithelial cell line (MCF-10A). The final reverse transcription reaction system was containing 200 ng of microRNA, 0.4 μl of 10 μM Primer 2 (U6 RT-Primer), 1 μl of TransScript RT/RI Enzyme SuperMix (Transgen, China), and 10 μl of 2× TS Reaction Mix (Transgen,

Table 1 Single-stranded DNA, primers, probes and templates sequences

Name	Sequence (5′ → 3′)
6-FAM-ssDNA	6-FAM-CCATGCTAATCTTCTCTGTATCGTTCCA
JOE-ssDNA	JOE-CCATGCTAATCTTCTCTGTATCGTTCCA
Cy3-ssDNA	Cy3-CCATGCTAATCTTCTCTGTATCGTTCCA
Primer 1	CTGCTTCGGCAGCACA
Primer 2	AACGCTTCACGAATTTGCGT
Primer 3	GCGCGTAGCAGCACAGAAAT
Primer 4	AGTGCAGGGTCCGAGGTATT
Probe 1	6-FAM-CCATGCTAATCTTCTCTGTATCGTTCCA-BHQ1
Probe 2	HEX-CACTGGATACGACGCCAATATTTCT-BHQ1
65 bp DNA	GTCGTATCCAGTGCAGGGTCCGAGGTATTCGCACTGGATACGACGCCAATATTTCTGTGCTGCTA
106 bp DNA	GTGCTCGCTTCGGCAGCACATATACTAAAATTGGAACGATACAGAGAAGATTAGCA TGGCCCCTGCGCAAGGATGACACGCAAATTCGTGAAGCGTTCCATATTTT

China) for a total volume of 25 μl. The reverse transcription cDNA was stored at −20 °C. Next, a direct PCR was carried out, containing 2 μl of reverse transcription cDNA, 0.5 μl of 10 μM Primer 1, 0.5 μl of 10 μM Primer 2, and 12.5 μl of 2× EasyTaq PCR SuperMix (Transgen, China) for a total volume of 25 μl. The direct PCR reaction process consisted in a pre-denaturation at 94 °C for 5 min, a denaturation at 94 °C for 5 s, an annealing at 60 °C for 30 s, an extension at 72 °C for 30 s for a total of 30 cycles, and a final extension at 72 °C for 5 min. Subsequently, a 2% agarose gel electrophoresis of 5 μl PCR products was performed, and a DiaSpin DNA Gel Extraction Kit (Diamond, China) was used to extract and purify the PCR products. The target fragments were ligated with pEASY-T3 Cloning Vector (Transgen, China), and then Trans1-T1 Phage Resistant Chemically Competent Cell (Transgen, China) was used for transformation of linkage products. The constructed plasmid was sent to Beijing TSINGKE Biological & Technology Company for identification and sequencing.

Fluorescence quenching of 6-FAM, JOE, and Cy3 by GOQDs

Initially, 1500 μl of 6-FAM-ssDNA (200 nM), JOE-ssDNA (200 nM), and Cy3-ssDNA (200 nM) solutions were separately inserted into three plastic tubes without nuclease, then 1500 μl of GOQDs working solution (26 μg ml^{-1}) were added. Successively, each tube was incubated at 37 °C for 30 min in the dark. Finally, the fluorescence intensity of the mixture was measured by a Lengguang F97PRO Fluorescence Spectrophotometer (Shanghai, China). The emission wavelengths and the excitation wavelengths of 6-FAM, JOE, and Cy3 were 520 nm and 494 nm, 548 nm and 520 nm, and 570 nm and 550 nm, respectively. Each measurement was repeated three times.

qRT-PCR method based on the GOQDs

A qRT-PCR experiment was carried out in an analytikJena qTOWER 2.2 Fluorescence Quantitative Gradient Polymerase Chain Reactor (Jena, Germany). When the TaqMan probe is cleaved by the Taq DNA polymerase during the qRT-PCR reaction, the fluorescent energy of the fluorophore cannot be adsorbed by the quenching group, thus a fluorescence signal is generated and can be used to monitor the amplification of the PCR.[23] The experiment showed that the final reaction systems contained 1 μl of template (106 bp or 65 bp DNA), 0.5 μl of 10 μM forward primer (Primer 1 or Primer 3), 0.5 μl of 10 μM reverse primer (Primer 2 or Primer 4), 12.5 μl of 2 × TransStart Probe qRT-PCR SuperMix (Transgen, China), and 0.5 μl of GOQDs solution for a total volume of 25 μl. The final concentration of the GOQDs in the reaction measured 0.00014 μg μl^{-1}. Moreover, the qRT-PCR reaction mixture without either 106 bp or 65 bp DNA but containing GOQDs was used as an internal control solution. The 106 bp plasmid DNA, the 65 bp DNA, and the GOQDs were then replaced by deionized water in a negative control solution. To define the optimal concentration of GOQDs, a quantity of 26 μg ml^{-1} was diluted into ultrapure water to prepare a series of working solutions with concentrations of 11 μg ml^{-1}, 5.3 μg ml^{-1}, 3.3 μg ml^{-1}, 2.2 μg ml^{-1}, and 1.5 μg ml^{-1} calculated *via* the concentration-absorbance standard curve. The 106 bp and 65 bp DNA was diluted into a working solution (10^{10} copies per μl) with ultrapure water. This solution was then continuously diluted to 10^9 to 10^1 copies per μl to generate a standard curve. The qRT-PCR reaction process consisted in a pre-denaturation of the sample at 94 °C for 30 s, which was followed by a denaturation at 94 °C for 5 s and annealing at 60 °C for 30 s for a total of 40 cycles. During each cycle and after the annealing process, the fluorescence emission intensity of the specimen at 520 nm or 580 nm was probed by using an excitation wavelength of 490 nm or 535 nm. 2% agarose gel electrophoresis of qRT-PCR products were performed and the measurements were repeated three times.

Statistical analyses

All statistical analyses were performed using the SPSS statistical package (Version 23.0; IBM Company, Chicago, IL, USA), as mean ± standard deviation (SD). *T* test were used to compare the treatment means with controls. The statistically significance level was set at $P < 0.01$.

Results and discussion

Improved Fenton reaction to prepare the GOQDs

To obtain high-quality GOQDs from graphite, three consecutive chemical reactions (intercalation, oxidation, and Fenton

reaction) are required. First, the intercalation reaction is dominated by the transformation of planar triangular MnO_3^+ into tetrahedral potassium permanganate under the action of sulphuric acid (95–98%). Graphite is oxidized and forms hydroxyl groups on the surface of the sample upon addition of the sulphuric acid. Furthermore, MnO_3^+, which is formed onto the GO surface, penetrates between the graphite carbon layers by exploiting the action of the hydroxyl group as intercalation agent.[24] After the intercalation process is completed, the planar triangular MnO_3^+ structure spontaneously transforms into a MnO_4 regular tetrahedral structure to support the graphite sheets.[25] Finally, a purple manganese-embedded graphite sample with a large MnO_4^- content is formed. Subsequently, upon the addition of H_2O_2 into the solution, the carbon atoms, which are present in the manganese-embedded graphite, react with the sulphuric acid to produce carbon dioxide, which dissolves in the water and forms HCO_3^-. Simultaneously, MnO_4^- can react directly with H_2O and graphite to form carbonate, bicarbonate, and manganese dioxide. Manganese dioxide reacts with the sulphuric acid and produces Mn^{2+}. The HCO_3^- ions, which are formed *via* these two mechanisms, react with H_2O_2 to produce percarbonate. Then, they interact with Mn^{2+} to form $[MnO]^{2+}$, which reacts with graphite to generate GO which contains a host of epoxy groups.[26,27]

Successively, the Fenton reaction occurs. The epoxy groups are attacked *via* hydroxyl radicals on the surface of GO and the GOQDs are obtained. The mixed solution undergoes an exothermic reaction and eventually boils upon the addition of zero-valent iron and H_2O_2 (30%), due to the presence of a large amount of hydroxyl radicals produced during the Fenton reaction. The carbon atoms, which are bound to the hydroxyl and epoxy groups on the surface of the graphene lamellae, are attacked by the large hydroxyl radicals, breaking the C–C bonds. Simultaneously, the newly formed oxygen-containing functional groups, such as the quinone groups, are attacked by the hydroxyl radicals.[28–30] In this fashion, the Fenton reaction induced by the presence of zero-valent iron and H_2O_2 (30%) can restart. An excessive presence of zero-valent iron reduces the –COOH on the surface of the GOQDs into –OH under acidic conditions. In this way, GOQDs sample rich in hydroxyl groups can be formed.

Characterization of GOQDs

The surface structure and size of the GOQDs were characterized *via* AFM (Fig. 1a–c). A statistical analysis of 120 samples shows that about 80% of the GOQDs are less than 3 nm thickness (Fig. 1c), indicating that most of the GOQDs are 1–3 layers, which is very close to that is reported in the previous papers.[31] In particular, the GOQDs prepared by the improved Fenton reaction can be freely dispersed in water with transparent appearance. In order to analyze the composition of the GOQDs, XPS experiments were carried out. Fig. 1d depicts the XPS spectrum: the C 1s peak consists of five features, which are located at 284.6 eV, 285.4 eV, 286.9 eV, 287.9 eV, and 289 eV and they correspond to the C=C, C–C, C–O, C=O, and –COOH characteristic peaks of the carbon skeleton, respectively.[32] It indicates that the sp^3 and sp^2 hybridization carbon atoms coexist in GOQDs. Moreover, the XPS results also suggest that a large amount of hydroxyl groups and epoxy groups are present on the surface of the GOQDs. The content of carbon and oxygen measures 53.77% and 39.27%, respectively and the ratio of carbon to oxygen is 1.37. The FT-IR spectrum of the GOQDs was also investigated (Fig. 1e). The peak at 1168 cm^{-1} corresponds to the characteristic absorption fingerprint of the epoxy (–O–) group,[33] whereas the feature at 1730 cm^{-1} is produced by the stretching vibration of the C=O group of the GOQDs.[34]

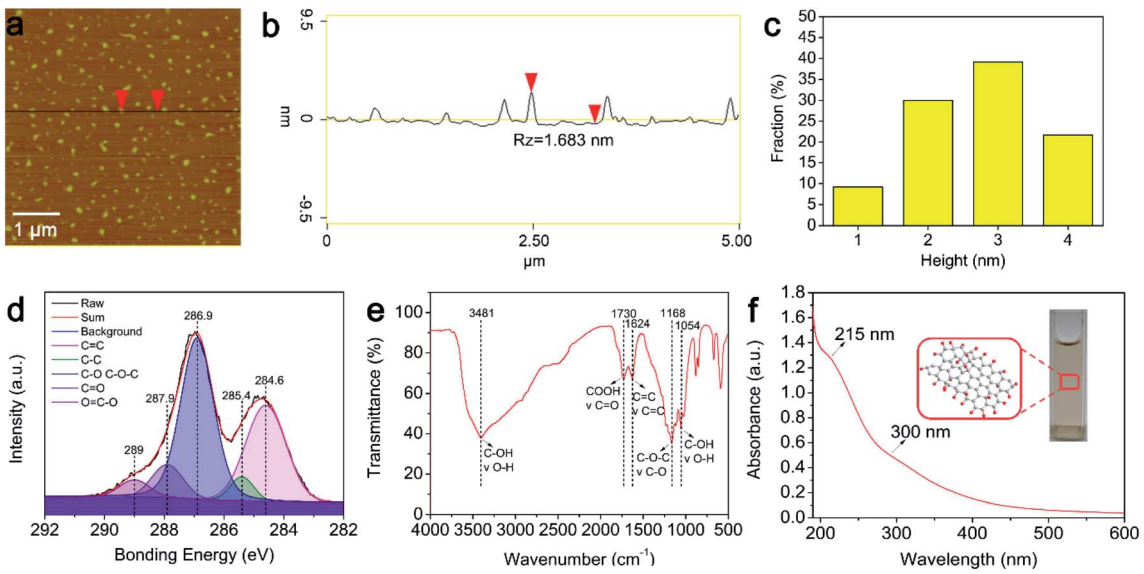

Fig. 1 Characterization of GOQDs. (a) AFM image of the GOQDs deposited on mica substrates. (b) Height profile of the GOQDs. (c) Height distribution of the GOQDs. (d) High-resolution XPS C 1s spectra of the GOQDs. (e) FT-IR spectra of GOQDs. (f) UV-vis absorption spectrum of GOQDs.

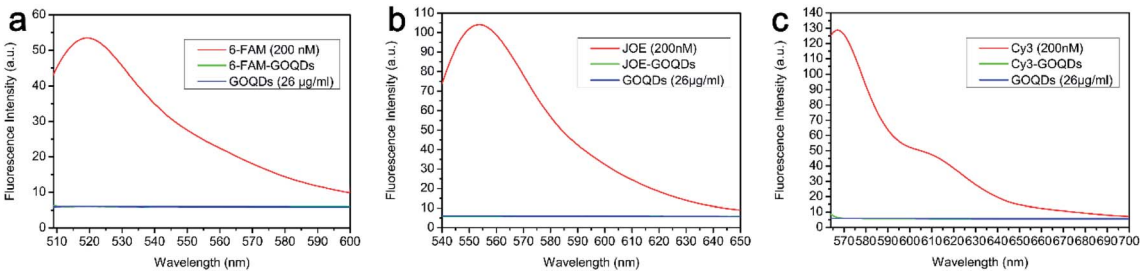

Fig. 2 Fluorescence quenching ability of GOQDs. (a) Fluorescence quenching of 6-FAM by GOQDs. (b) Fluorescence quenching of JOE by GOQDs. (c) Fluorescence quenching of Cy3 by GOQDs.

Moreover, a wide and strong absorption peak appears in the 3250–3750 cm^{-1} range. This feature is attributed to the stretching vibration of the –OH group.[35] FT-IR spectroscopy implies that these functional groups induce excellent hydrophilic properties in the GOQDs sample. Based on the UV-vis results (Fig. 1f), the absorption peak at 215 nm is attributed to the $\pi \rightarrow \pi^*$ transition of the sp^2 C–C bonds.[14] Furthermore, the $n \rightarrow \pi^*$ transition of the C=O bonds or other functional groups on the surface of the GOQDs present a shoulder peak in approximately 300 nm.[36] In order to better understand luminescence characteristics of the GOQDs, the luminescence spectrum and photoluminescence excitation spectrum measurements were carried out. Fig. 2 illustrated the luminescence spectrum of the GOQDs. One can see that the synthesized GOQDs show no significant variation in the fluorescence intensity upon ultraviolet and visible light excitations.

Fluorescence quenching of 6-FAM, JOE, and Cy3

In order to explore the properties of the GOQDs and illustrate their fluorescence quenching effect, they were incubated with three different fluorescent dyes. The emission wavelengths of the fluorescent dyes 6-FAM, JOE, and Cy3 are 520 nm, 548 nm, and 570 nm, respectively. As shown in Fig. 2, the fluorescence intensity of these three dyes decreases after the addition of the GOQDs, indicating that their effective quenching effect on the fluorescence of the group. The sp^2 aromatic structure of GO can adsorb the ssDNA *via* its π–π stacking cloud.[18,37–39] For this reason, even a very small layer of GO can bond with the base of the fluorescent probe *via* such π–π cloud. In addition, the hydroxyl groups on the surface of GOQDs can also form hydrogen bonds with the base of the fluorescent probe, promoting the adsorption of the fluorescent probe equally. Ultimately, FRET occurs between the fluorescent probe and the GOQDs. The fluorescent group on the probe acts as a donor to transfer the energy to the GOQDs, which results in a fluorescence quenching effect.[10] Additionally, the combination of the characterization data and the literature shows that the background fluorescence intensity of GOQDs prepared *via* the improved Fenton reaction is much lower than for traditional GOQDs (Fig. 2).[40] According to the literature, the higher the –COOH content on the surface of the GOQDs is, the stronger is the fluorescence intensity of the GOQDs. However, when –COOH is reduced into –OH a reduction of its fluorescence intensity can be detected.[28] The reasons for low background fluorescence intensity of GOQDs were strongly supported by the results of XPS, FT-IR and UV-vis. The results also suggest that the GOQDs may have potential applications in the clinical disease detection field and may be used in qRT-PCR as an effective fluorescence quencher to detect target genes.

Screening the optimal concentration of GOQDs in qRT-PCR

The qRT-PCR is a highly sensitive method for DNA quantitative analysis. In this experiment, the effects of the GOQDs on the qRT-PCR process were investigated by adding GOQDs in different concentrations into a traditional qRT-PCR system. To avoid the contributions of the different templates into the estimate of the qRT-PCR amplification efficiency, 106 bp plasmid DNA and synthesized 65 bp DNA was used as the templates.

During the qRT-PCR process, the amplification curve changes as the concentrations of GOQDs decreases (Fig. 3a and b). Moreover, the curve resembles a typical amplification control curve with an optimal concentration of GOQDs of 5.3 μg ml^{-1} (106 bp and 65 bp). The agarose gel electrophoresis results are consistent with the trend of the amplification curve and indicate that the excess of GOQDs can inhibit the qRT-PCR amplification reaction by adsorbing a high quantity of the probe, primer, or template through its sp^2 conjugated region. Moreover, when the concentration of the GOQDs is below the optimal concentration (5.3 μg ml^{-1}), a host in the non-specific amplification occurs in the qRT-PCR system of 106 bp plasmid DNA. Contrarily, the specificity of the qRT-PCR process increases upon the increase of the GOQDs concentrations. The results suggested that GOQDs could improve qRT-PCR specificity in the concentration range of 5.3–11 μg ml^{-1}. Additionally, a concentration of GOQDs of 5.3 μg ml^{-1} is an optimal concentration to maintain high specificity in our qRT-PCR system (106 bp and 65 bp).

Specificity of qRT-PCR based on GOQDs

To further understand the effect of the GOQDs on the TaqMan qRT-PCR process, agarose gel electrophoresis was performed after qRT-PCR. As shown in Fig. 3a, the non-specific amplification bands disappear upon the addition of GOQDs (>5.3 μg ml^{-1}). During the qRT-PCR process, when the dNTPs, the cDNA polymerase, and the template are mixed, the background signals generated by the non-specific amplification appear even

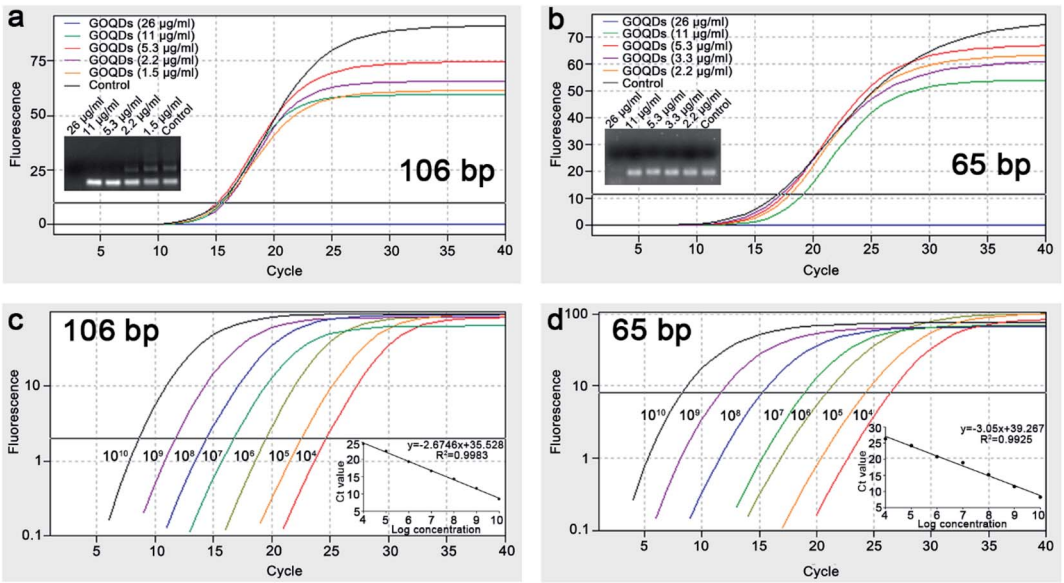

Fig. 3 Screening the optimal concentration of GOQDs and the sensitivity and specificity of qRT-PCR. (a) qRT-PCR amplification curve of 106 bp plasmid DNA after addition of 26 μg ml^{-1}, 11 μg ml^{-1}, 5.3 μg ml^{-1}, 2.2 μg ml^{-1} and 1.5 μg ml^{-1} GOQDs, the inset figure was the result of agarose gel electrophoresis. (b) qRT-PCR amplification curve of 65 bp DNA after addition of 26 μg ml^{-1}, 11 μg ml^{-1}, 5.3 μg ml^{-1}, 3.3 μg ml^{-1} and 2.2 μg ml^{-1} GOQDs, the inset figure was the result of agarose gel electrophoresis. (c) The amplification plots of 106 bp plasmid DNA. The inset figure is a standard curve of 106 bp plasmid DNA amplification with a determining coefficient of 0.9983. (d) The amplification plots of 65 bp DNA. The inset figure is a standard curve of 65 bp DNA amplification with a determining coefficient of 0.9925.

if the enzyme is not heat-activated.[41] Due to the lack of a biofeedback mechanism *in vitro*, the effect of the GOQDs on the specificity of qRT-PCR may be the result of the interaction of multiple factors. Therefore, we assume that the enhancement effects of GOQDs can be explained as follows. First, after the optimal concentration of GOQDs is achieved, the large number

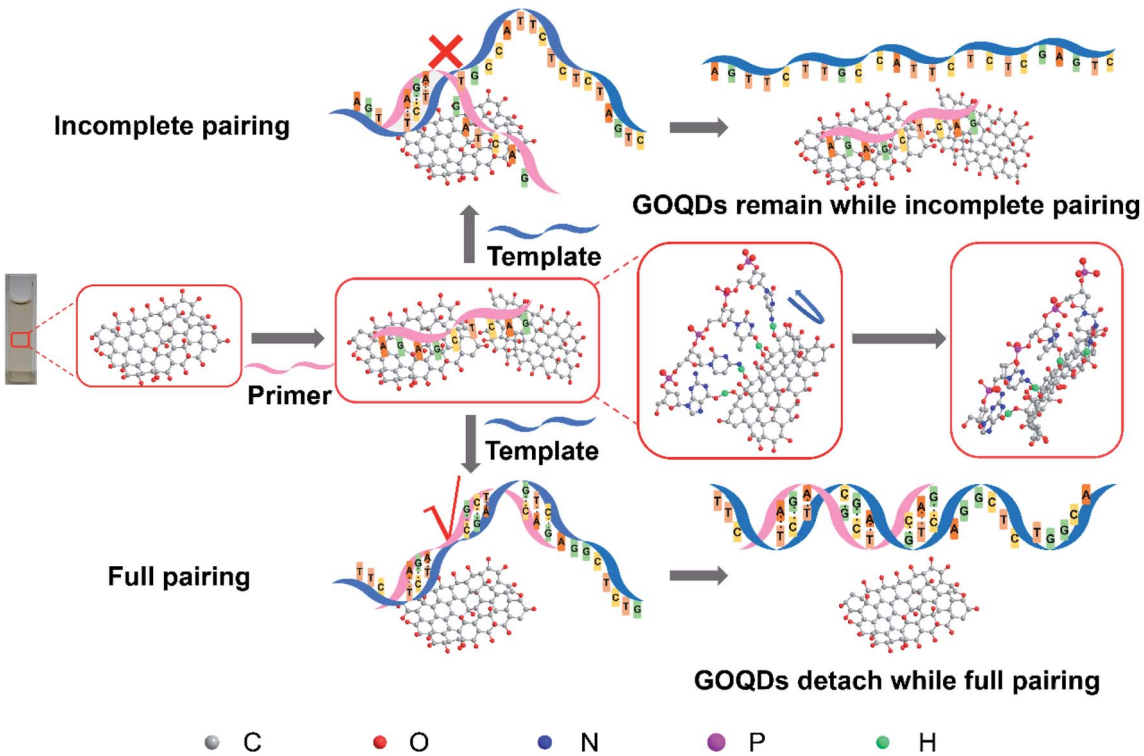

Fig. 4 Scheme of enhancing qRT-PCR specificity by GOQDs. The whole picture shows the schematic diagram of the hypothesis of enhancing qRT-PCR specificity by GOQDs.

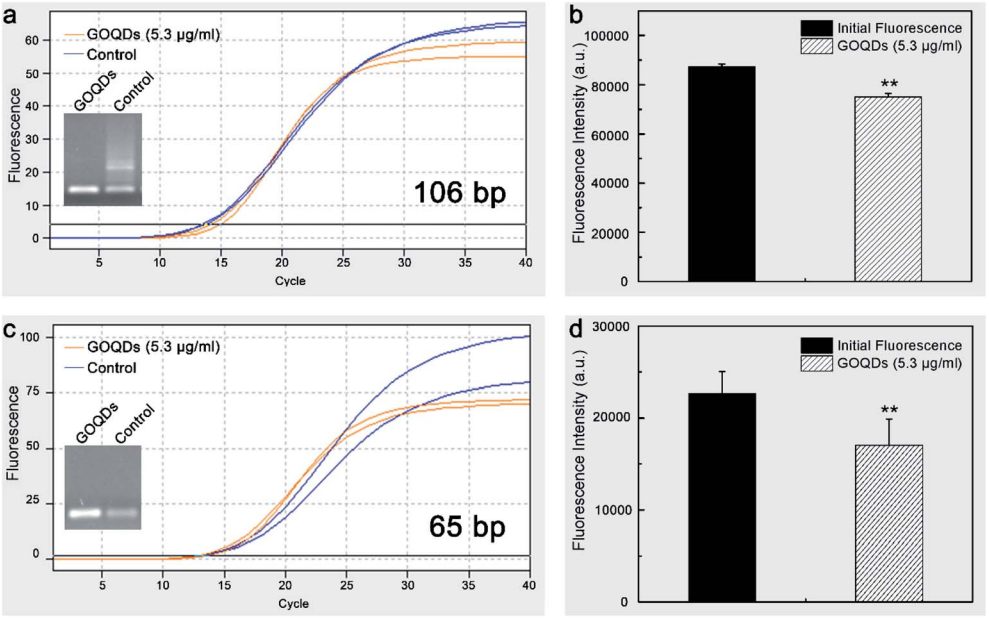

Fig. 5 Detection of two different lengths of DNA sequences by qRT-PCR based on GOQDs. (a) qRT-PCR amplification curve of 106 bp plasmid DNA after addition of 5.3 μg ml^{-1} GOQDs, the inset figure was the result of agarose gel electrophoresis. (b) Fluorescence quenching results of Probe 1 with 5.3 μg ml^{-1} GOQDs. (c) qRT-PCR amplification curve of 65 bp DNA after addition of 5.3 μg ml^{-1} GOQDs, the inset figure was the result of agarose gel electrophoresis. (d) Fluorescence quenching results of Probe 2 with 5.3 μg ml^{-1} GOQDs.

of hydroxyl groups on the surface of GOQDs may interact with the primers to form hydrogen bonds and the π–π stacking can form together, thereby inhibiting the mismatches between the primers and the templates at the non-target sites. When the primers are fully paired with the templates, a qRT-PCR reaction can occur due to detachment of the primers from the surface of GOQDs. This may reduce the non-specific amplification products (Fig. 4). Second, the GOQDs, which are added into the system, can interact with excessive probes, primers, or templates, reducing the binding of primers to the templates to inhibit the occurrence of non-specific reactions. Herein, the addition of GOQDs in the qRT-PCR reaction can reduce the non-specific amplification process and improve the specificity of the qRT-PCR method. In addition, an increase in the concentration of the GOQDs resulted in an enhancement in the adsorption of the GOQDs on the primers. At the same time, due to the existence of the above two mechanisms, the specificity of qRT-PCR can be scarcely improved by the increase of the GOQDs concentrations. However, it can be largely inhibited by GOQDs upon addition of >11 μg ml^{-1}. The possible reason could be that the adsorption capacity of GOQDs for the primers are far stronger than the complementary pairing ability of the primers and the templates.

Sensitivity of qRT-PCR based on GOQDs

Under the optimal concentration of GOQDs (5.3 μg ml^{-1}), the detection performance of this qRT-PCR method was evaluated by adding varying concentrations of the DNA templates into the qRT-PCR system. As shown in Fig. 3c and d, the C_t value decreases upon the decrease of the DNA copy number. The standard curve shows that the C_t value is linear as a function of the logarithm of the initial 106 bp plasmid DNA and 65 bp DNA templates copy number in the 10^4 to 10^{10} copies per μl range with a determining coefficient of 0.9983 and 0.9925. According to the theory,[42] a quantitative relationship can be established between the initial copy number of the DNA templates and the amount of PCR product at any cycle. Therefore, the qRT-PCR method based on the GOQDs allows on to detect the DNA in a wide range of DNA copy number and the detection range is higher than 7 orders of magnitude with a detection limit of 10^4 copies per μl. This is the first time to achieve sensitive analysis of DNA using the qRT-PCR method based on the GOQDs.

Detection of 106 bp and 65 bp DNA by qRT-PCR based on GOQDs

The effect of the GOQDs on the qRT-PCR amplification was further investigated by detecting two different lengths of DNA sequences (106 bp and 65 bp). Typical qRT-PCR results obtained by using the GOQDs are shown in Fig. 5. Upon the addition of the GOQDs (5.3 μg ml^{-1}) into the two qRT-PCR systems, a significant reduction in the background fluorescence intensity of the TaqMan probes of 20% ($P = 0.0006 < 0.01$) and 25% ($P = 0.0014 < 0.01$) can be observed (Fig. 5b and d). However, the plateau of the amplification curves is lower than that of the control groups (Fig. 5a and c), probably due to the formation of the π–π stacking between the fluorophores and the GOQDs to trigger FRET after the TaqMan probe was hydrolyzed by the Taq DNA polymerase. This, in fact, generates a quenching mechanism on the fluorescence intensity of several fluorescent groups under the action of the GOQDs. The improved specificity of qRT-PCR by GOQDs indicates that the GOQDs-based qRT-PCR method can be used to detect DNA specifically and selectively.

Conclusions

In summary, GOQDs, rich in hydroxyl groups and with a low background fluorescence intensity, were prepared *via* the improved Fenton reaction to efficiently quench the fluorescence of three fluorescent dyes (6-FAM, JOE, and Cy3). In this study, a simple and effective qRT-PCR method was established to evaluate the effect of the GOQDs. The results show that the GOQDs effectively decrease the background fluorescence intensity of the TaqMan probe, reduce the non-specific amplification, and improve the specificity of the qRT-PCR reaction. Furthermore, the qRT-PCR method based on the GOQDs can detect the 106 bp and 65 bp DNA in a concentration of 10^4 copies per μl, in a linear range of 10^4 to 10^{10} copies per μl and with a detection range spanning 7 orders of magnitude. This technique can also detect two different lengths of DNA sequences with a high specificity. These results indicate that the GOQDs prepared by using the improved Fenton reaction are promising materials to develop an efficient qRT-PCR method for a high-specific and selective detection of DNA.

Conflicts of interest

There are no conflicts to declare.

Acknowledgements

This study was financially supported by the Outstanding Youth Science Foundation of Sichuan Province (Grant No. 2017JQ0015), by project first-class disciplines development supported by Chengdu University of Traditional Chinese Medicine (Grant No. CZYJC1904), by scientific research fund of Sichuan provincial education department (Grant No. 18CZ0010). We thank the Innovative Institute of Chinese Medicine and Pharmacy at Chengdu University of Traditional Chinese Medicine for its instrumental support (PL, FT-IR, and vacuum freeze drier).

Notes and references

1 S. Ellairaja, N. Krithiga, S. Ponmariappan and V. S. Vasantha, *J. Agric. Food Chem.*, 2017, **65**, 1802–1812.
2 Y. T. Yew, A. H. Loo, Z. Sofer, K. Klímová and M. Pumera, *Appl. Mater. Today*, 2017, **7**, 138–143.
3 C. Lungu, S. Pinter, J. Broche, P. Rathert and A. Jeltsch, *Nat. Commun.*, 2017, **8**, 649.
4 L. Andreeva, B. Hiller, D. Kostrewa, C. Lässig, C. C. de Oliveira Mann, D. J. Drexler, A. Maiser, M. Gaidt, H. Leonhardt, V. Hornung and K. P. Hopfner, *Nature*, 2017, **549**, 394–398.
5 A. H. Loo, Z. Sofer, D. Bouša, P. Ulbrich, A. Bonanni and M. Pumera, *ACS Appl. Mater. Interfaces*, 2016, **8**, 1951–1957.
6 Z. S. Qian, X. Y. Shan, L. J. Chai, J. J. Ma, J. R. Chen and H. Feng, *Biosens. Bioelectron.*, 2014, **60**, 64–70.
7 R. M. Kong, X. B. Zhang, Z. Chen and W. H. Tan, *Small*, 2011, **7**, 2428–2436.
8 T. Sun, N. Xia and L. Liu, *Nanomaterials*, 2016, **6**, 20.
9 Y. W. Lin, C. C. Huang and H. T. Chang, *Analyst*, 2011, **136**, 863.
10 D. M. Kim, D. H. Kim, W. Jung, K. Y. Lee and D. E. Kim, *Analyst*, 2018, **143**, 1797–1804.
11 R. V. Goreham, K. L. Schroeder, A. Holmes, S. J. Bradley and T. Nann, *Mikrochim. Acta*, 2018, **185**, 128.
12 S. Y. Choi, S. H. Baek, S. J. Chang, Y. Song, R. Rafique, K. T. Lee and T. J. Park, *Biosens. Bioelectron.*, 2017, **93**, 267.
13 R. Gao, Z. Zhong, X. Gao and L. Jia, *J. Agric. Food Chem.*, 2018, **66**, 10898–10905.
14 S. Ahirwar, S. Mallick and D. Bahadur, *ACS Omega*, 2017, **2**, 8343–8353.
15 F. Zhang, F. Liu, C. Wang, X. Xin, J. Liu, S. Guo and J. Zhang, *ACS Appl. Mater. Interfaces*, 2016, **8**, 2104–2110.
16 Y. Liu, Y. Xu, X. Geng, Y. Huo, D. Chen, K. Sun, G. Zhou, B. Chen and K. Tao, *Small*, 2018, **14**, 1800293.
17 E. Lai, *Anal. Biochem.*, 2016, **5**, e165.
18 Y. He, B. Zhang and Z. Fan, *Mikrochim. Acta*, 2018, **185**, 163.
19 L. M. Zhang, T. Jiang, X. F. Li, Y. Wang, C. Zhao, S. Zhao, L. Xi, S. J. Zhang, X. Z. Liu, Y. J. Jia, H. Yang, J. P. Shi, C. X. Su, S. X. Ren and C. C. Zhou, *Cancer*, 2017, **123**, 2927–2935.
20 T. S. Kang, *Trends Food Sci. Technol.*, 2019, **91**, 574–585.
21 A. Nakashima, N. Ihara, M. Shigeta, H. Kiyonari, Y. Ikegaya and H. Takeuchi, *Science*, 2019, **365**, eaaw5030.
22 I. Baris, O. Etlik, V. Koksal, Z. Ocak and S. T. Baris, *Anal. Biochem.*, 2013, **441**, 225–231.
23 S. Mocellin, C. R. Rossi, P. Pilati, D. Nitti and F. M. Marincola, *Trends Mol. Med.*, 2003, **9**, 189–195.
24 D. J. Royer, *J. Inorg. Nucl. Chem.*, 1961, **17**, 159–167.
25 X. Hu, L. Shi, D. Zhang, X. Zhao and L. Huang, *RSC Adv.*, 2016, **6**, 14192–14198.
26 B. S. Lane, M. Vogt, V. J. DeRose and K. Burgess, *J. Am. Chem. Soc.*, 2002, **124**, 11946–11954.
27 M. M. Najafpour, F. Rahimi, M. Amini, S. Nayeri and M. Bagherzadeh, *Dalton Trans.*, 2012, **41**, 11026–11031.
28 X. Zhou, Y. Zhang, C. Wang, X. Wu, Y. Yang, B. Zheng, H. Wu, S. Guo and J. Zhang, *ACS Nano*, 2012, **6**, 6592–6599.
29 H. Bai, W. Jiang, G. P. Kotchey, W. A. Saidi, B. J. Bythell, J. M. Jarvis, J. M. Jarvis, A. G. Marshall, R. A. Robinson and A. Star, *J. Phys. Chem. C*, 2014, **118**, 10519.
30 X. Zhou and L. Xu, *Chem. Res. Chin. Univ.*, 2017, **33**, 1–6.
31 F. Shi, Y. Zhang, W. Na, X. Zhang, Y. Li and X. Su, *J. Mater. Chem. B*, 2016, **4**, 3278–3285.
32 L. Tang, R. Ji, X. Cao, J. Lin, H. Jiang, X. Li, K. S. Teng, C. M. Luk, S. Zeng, J. Hao and S. P. Lau, *ACS Nano*, 2012, **6**, 5102–5110.
33 M. Balaji, S. Jegatheeswaran, P. Nithya, P. Boomi, S. Selvam and M. Sundrarajan, *J. Photochem. Photobiol., B*, 2018, **178**, 371–379.
34 P. Routh, S. Das, A. Shit, P. Bairi, P. Das and A. K. Nandi, *ACS Appl. Mater. Interfaces*, 2013, **5**, 12672–12680.
35 D. W. Lee, V. L. De Los Santos, J. W. Seo, L. L. Felix, D. A. Bustamante, J. M. Cole and C. H. W. Barnes, *J. Phys. Chem. B*, 2010, **114**, 5723–5728.
36 Q. J. Lu, C. Y. Wu, D. Liu, H. Y. Wang, W. Su, H. T. Li, Y. Y. Zhang and S. Z. Yao, *Green Chem.*, 2017, **19**, 900–904.

37 N. Duan, S. Wu, S. Dai, T. Miao, J. Chen and Z. Wang, *Microchim. Acta*, 2014, **182**, 917–923.
38 X. Cui, L. Zhu, J. Wu, Y. Hou, P. Wang, Z. Wang and M. Yang, *Biosens. Bioelectron.*, 2015, **63**, 506–512.
39 Z. Liu and X. Su, *Biosens. Bioelectron.*, 2017, **87**, 66–72.
40 F. Liu, M. H. Jang, H. D. Ha, J. H. Kim, Y. H. Cho and T. S. Seo, *Adv. Mater.*, 2013, **25**, 3657–3662.
41 E. Tan, B. Erwin, S. Dames, T. Ferguson, M. Buechel, B. Irvine, K. Voelkerding and A. Niemz, *Biochemistry*, 2008, **47**, 9987–9999.
42 K. Roh, D. M. Kim, E. H. Lee, H. Kim, H. S. Park, J. H. Jang, S. H. Hwang and D. E. Kim, *Chem. Commun.*, 2015, **51**, 6960–6963.

